Preprints (www.preprints.org) | NOT PEER-REVIEWED | Posted: 23 January 2018 doi:10.20944/preprints201801.0208.v1

Peer-reviewed version available at Energies 2018, 11, 595; doi:10.3390/en11030595

1 *Article*

2 A High-Precision Adaptive Thermal Network Model 3 for Monitoring the Junction Temperature of IGBTs

4 **Ning An[1], Mingxing Du [1]*, Zhen Hu[2] and Kexin Wei[1,]**

5 [1] Tianjin key laboratory of control theory & applications in complicated system, Tianjin University of
6 Technology, Tianjin, China; dumx@tjut.edu.cn
7 [2] School of electrical engineering and automation, Tianjin University, Tianjin, China
8 * Correspondence: dumx@tjut.edu.cn; Tel.: +86-22-60214268

9 **Abstract:** This paper proposes a novel method for optimizing the Cauer-type thermal network
10 model considering both the temperature influence on the extraction of parameters and the errors
11 caused by the physical structure. In terms of prediction of the transient junction temperature and
12 the steady-state junction temperature, the parameters of conventional Cauer-type are modified, and
13 the general method for estimating junction temperature is studied by using the adaptive thermal
14 network model. The results show that junction temperature estimated by adaptive Cauer-type
15 thermal network model is more accurate than that of the conventional model.

16 **Keywords:** Insulated gate bipolar transistor (IGBT); thermal network; parameter identification;
17 junction temperature
18

19 1. Introduction

20 As a key component in the modern power-electronic system, insulated gate bipolar transistors
21 (IGBTs) are widely used in high-reliability systems [1] and play a significant role in wind turbines [2-
22 3], aircraft [3-4], electric vehicle [5-7], etc. The reason for the widespread application of IGBTs lies in
23 IGBTs' excellent performance in the aspects of switching frequency, energy efficiency, power density
24 and cost effectiveness [8]. Simultaneously, higher quality is required with more formidable working
25 conditions and stricter operating conditions. Almost 60% of power equipment failure resulted higher
26 junction temperature caused by heat and increase of the thermal resistance or extra power loss,
27 according to relevant data [9-10]. The reliability research of semiconductors depends on accurate
28 measurement of the junction temperature. Consequently, the junction temperature of the IGBT is
29 considered as one of important indices for its health and reliability.
30 The accurate junction temperature is the important foundation of virtual simulation, precise
31 design and practice. The main prediction methods of junction temperature involve infrared camera
32 detection, thermal-sensitive electrical parameters (TSEPs) and electrothermal network models. The
33 most obvious advantage of infrared camera detection lies in the capturing of the temperature field;
34 however, the IGBT's package must be removed during the measuring [11]. Regarding the TSEPs, on-
35 state voltage ($V_{ce\text{-}on}$) [12], gate threshold voltage (V_{ge}) [13], turn-on time (t_{on}) [14], turn-off time (t_{off})
36 [15] and other electrical parameters will contribute to the prediction of the junction temperature.
37 However, circuitry design would be more complicated with the higher precision required, making
38 this method quite expensive [16]. The last method, the use of the electrothermal network model, can
39 provide accurate transient junction temperature and steady-state junction temperature information,
40 thereby enabling on-line monitoring of the junction temperature without a complicated measuring
41 circuit. Hence, the electrothermal network model is extensively used and shows prospects for further
42 development [17].
43 The current studies of the resistance-capacitance (RC) thermal network are divided into the use
44 of the Foster-type and Cauer-type models; the Foster-type model is based on the measurement of the
45 temperature dynamics of power devices [18], and the Cauer-type model is based on the physical
46 structure of the device and is considered to be a relatively accurate model of the thermal behaviours

© 2018 by the author(s). Distributed under a Creative Commons CC BY license.

Preprints (www.preprints.org) | NOT PEER-REVIEWED | Posted: 23 January 2018 doi:10.20944/preprints201801.0208.v1

Peer-reviewed version available at Energies 2018, 11, 595; doi:10.3390/en11030595

47 of IGBTs [19-20]. In [21], a Foster-type model was introduced for the IGBTs used in a three-phase
48 inverter. To solve the thermal coupling effects among the chips, the three-dimensional RC-lumped
49 thermal networks were proposed [22-23]. As such, a dynamic electrothermal model extended to a
50 paralleled system was proposed to establish a transient model to characterize the relationship
51 between power losses and junction temperature [24]. One problem with the Foster-type thermal
52 network is that its parameters are based on mathematical fitting of the measured/simulated junction
53 temperature curves, and each of the RC-lumped elements in the Foster-type network has no physical
54 meaning. Therefore, the Cauer-type model was proposed to obtain the temperature distribution of
55 each layer. In [25], a Cauer-type model to monitor an IGBT's health condition was presented. The
56 thermal model consisting of a three-dimension network of RC cells constructed for time-dependent
57 operation was proposed [26]. Malberti [27] introduced the Elmore delay equation to model the
58 propagation delay times of the heat flux in the layers of IGBT. However, some problems were ignored
59 in these studies: a) based on the extraction of parameters at constant temperature, without
60 considering the temperature dependence of the thermal conductivity and the specific heat capacity,
61 the deviation of Cauer-type model will be amplified at certain temperatures; b) the transient thermal
62 behaviour of the IGBT is oversimplified by treating each layer as a block with uniform temperature
63 distribution, resulting in poor prediction performance of the model.
64 On the basis of the previous analysis, this paper proposes the optimization of the adaptive
65 temperature Cauer-type network model. The optimization lies in
66 a) Obvious improvement of the accuracy of the prediction of the steady-state junction
67 temperature, considering the influence of temperature.
68 b) Efficient improvement of the prediction performance of the transient junction temperature by
69 redefining the hierarchical Cauer-type architecture for the internal structure of the module.
70 The updated network not only strongly improves the accuracy of the estimated transient
71 junction temperature variation for IGBTs but also highly contributes to optimizing the prediction
72 performance of the steady-state junction temperature.
73 This paper is organized as follows. Section 2 presents an analysis of the deviation of the model
74 based on the materials properties and physical structures successively to perform optimization
75 accordingly. Section 3 verifies the efficiency of the model via simulation experiment. Section 4 shows
76 the validation of the simulation results in practice.

77 **2. Methods**

78 The basic structure of IGBT and its conventional lumped Cauer-type thermal network model are
79 shown in Figure 1. Figure 1 (a) shows the seven-level sandwich structure of the IGBT module from
80 chip to baseplate. Figure 1 (b) shows a circuit used to establish a complete seven-order IGBT heat
81 transfer network structure on the basis of the theory of electrothermal analogy. For each layer, the
82 thermal resistance R_{th} and thermal capacitance C_{th} are calculated using the equations below:

83 $$R_{th} = \int_0^d \frac{1}{k \cdot A(z)} dz \quad (1)$$

84 $$C_{th} = \int_0^d c \cdot \rho \cdot A(z) dz \quad (2)$$

85 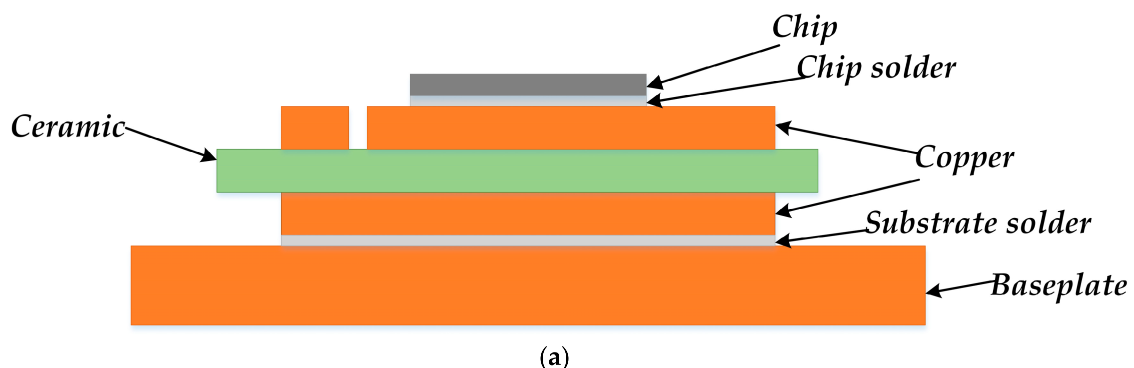

86 (a)

Preprints (www.preprints.org) | NOT PEER-REVIEWED | Posted: 23 January 2018 doi:10.20944/preprints201801.0208.v1

Peer-reviewed version available at Energies 2018, 11, 595; doi:10.3390/en11030595

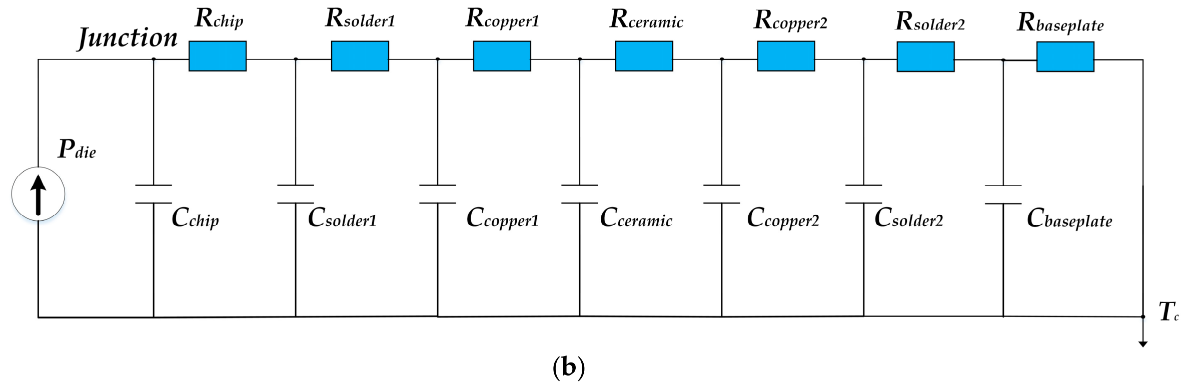

87
88 (**b**)

89 **Figure 1.** (**a**) Sandwich structure of IGBT; (**b**) Cauer-type thermal model.

90 Where d_i is the thickness of the i_{th} layer, k_i is the thermal conductivity of the i_{th} layer, c_i is the
91 specific heat capacity of the i_{th} layer, ρ_i is the density of the i_{th} layer material, and A(z) is the effective
92 cross-sectional area of the i_{th} layer. Based on the conventional lumped Cauer-type model, the
93 improved method proposed in this paper is conducted using the following two steps:

94 • Establish the Cauer-type thermal network of the non-constant thermal conductivity and the
95 specific heat capacity

96 The conventional lumped Cauer-type model does not take into account the effect of operating
97 environment temperature on the internal material properties. The thermal resistance of the IGBT
98 power module is determined by the thermal conductivity, and the thermal conductivity is a variable
99 related to the temperature. Similarly, the thermal capacitance is determined by the specific heat
100 capacity, which is also a temperature-dependent variable. In the process of establishing the model,
101 the effect of temperature on its parameters will be considered to improve the accuracy of the
102 prediction of the junction temperature. According to the literature [28-29], the relationship between
103 thermal conductivity and specific heat capacity of different materials and temperature can be
104 obtained. After fitting the data with the least square method, the approximate expressions of thermal
105 conductivity and heat capacity of materials are obtained, as shown in figure [2-3] below.

106 $$y = ax^2 + bx + c \quad (3)$$

107 $$y = ax^b \quad (4)$$

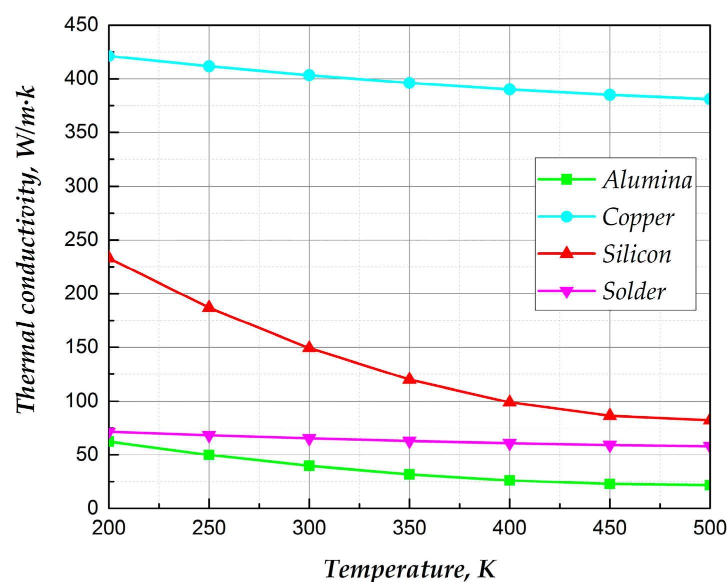

108
109 **Figure 2.** The relationship between thermal conductivity and temperature of different materials.

Preprints (www.preprints.org) | NOT PEER-REVIEWED | Posted: 23 January 2018 doi:10.20944/preprints201801.0208.v1

Peer-reviewed version available at Energies 2018, 11, 595; doi:10.3390/en11030595

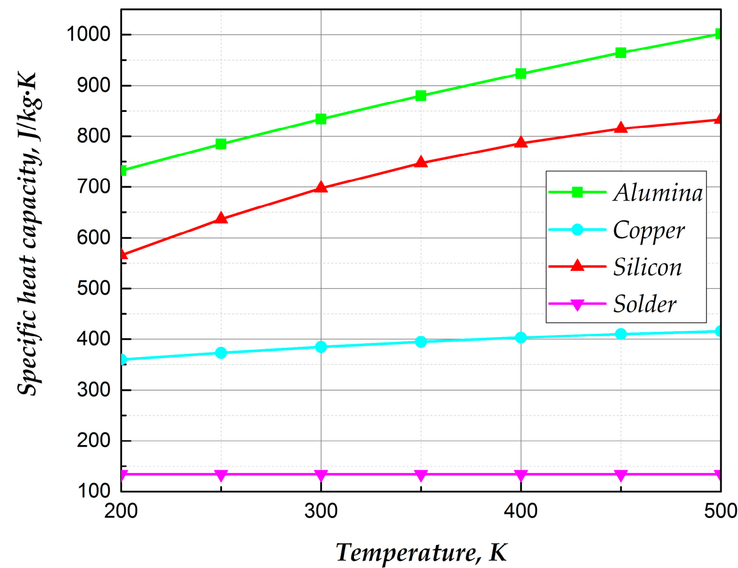

Figure 3. The relationship between specific heat capacity and temperature of different materials.

After considering the nonlinear temperature behaviour of a material, equations (1) and (2) are improved to be:

$$R_{th} = \int_0^d \frac{1}{k(T)\cdot A(z)} dz \tag{5}$$

$$C_{th} = \int_0^d c(T)\cdot \rho \cdot A(z) dz \tag{6}$$

According to equations (5) and (6), the heat transfer network with non-constant thermal conductivity and specific heat capacity is established; the accuracy of the model has been significantly improved. To further improve the accuracy of the model, this paper will optimize the physical structure of the Cauer-type model.

- Optimization of the Cauer-type model based on the physical structure

Although the seven-layer Cauer-type model established by the seven-layer physical structure of the IGBT power module has a high computational efficiency, the higher thermal resistance and higher thermal capacitance of the ceramic layer and the baseplate layer in the thermal network model lead to a longer time constant, which, in turn, results in the decrease in the model prediction of the overall junction temperature performance; as a result, it does not accurately capture the dynamic junction temperature changes of the IGBT module during the power cycle. Based on the seven-layer Cauer-type thermal network structure of the IGBT module, this paper analyses the operating characteristics of a single-layer RC network and compares the interaction between the layers of different time scales to establish the accurate prediction of the IGBT transient junction temperature using the heat transfer model. The single-level Cauer-type model is shown in figure 4 below:

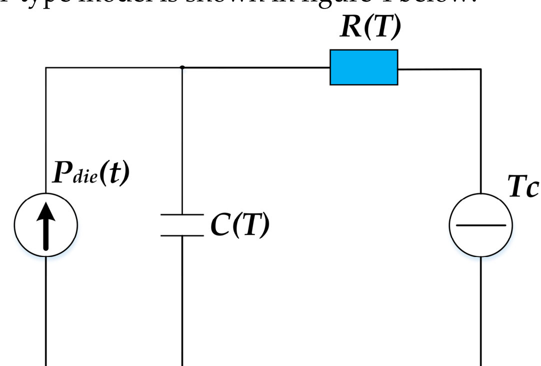

Figure 4. Single-layer Cauer-type thermal network.

Preprints (www.preprints.org) | NOT PEER-REVIEWED | Posted: 23 January 2018 doi:10.20944/preprints201801.0208.v1

Peer-reviewed version available at Energies 2018, 11, 595; doi:10.3390/en11030595

By using the electrothermal analogy method, the complete response of the first order equation of the single-layer Cauer-type thermal network is as follows:

$$T_{jc} = T_j - T_c = (T_{js} - T_c)\left(1 - e^{-\frac{t}{\tau}}\right) \tag{7}$$

$$\tau = R(T)C(T) \tag{8}$$

T_{js} is the steady-state junction temperature, T_{jc} is the temperature difference between the chip and the case, T_j is the junction temperature, T_c is the case temperature, and τ is the time constant. According to equation (7), the time required for junction temperature to reach steady state is given by:

$$t = -\tau \ln\left(1 - \frac{T_j - T_c}{T_{js} - T_c}\right) \tag{9}$$

When T_{jc}=0.98T_{js}, the system is defined as the steady state; thus,

$$t = -\tau \ln 0.02 \tag{10}$$

This paper takes the SKM75GB12T4 module of SEMIKRON Company as the research object. The specific dimensions of the module and the material properties are shown in Table 1

Table 1. Parameters of the IGBT module (SKM75GM12T4).

Material layer	Thickness (mm)	Density (kg/m³)	Length (mm)	Width (mm)
Silicon	0.15	2329	7.24	6.9
Solder	0.12	7300	7.24	6.9
Copper	0.3	8960	28.5	25.8
Alumina	0.38	3780	30.65	28
Copper	0.3	8960	28.5	25.8
Solder	0.12	7300	28.5	25.8
Copper	2.8	8960	91.4	31.4

Based on equations (5) and (6), the values and distribution of the time constant of each layer under ambient temperature (25℃) are shown in Figure 5:

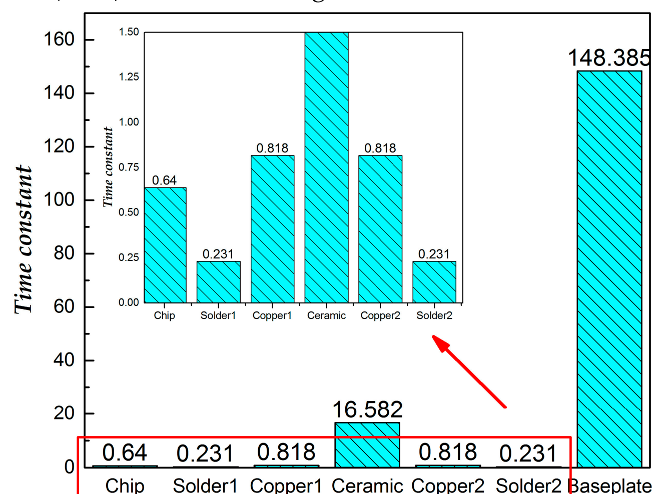

Figure 5. Time constant of each layer.

In the heat transfer model, the RC is a constant for the transition time of the network and is the physical parameter reflecting the time required to transfer the heat over the layer. The larger the time constant is, the longer the time it takes to transfer the heat over the layer. Equation (9) is used to solve the values and distribution of the time constant for each layer to obtain the steady-state under ambient temperature (25℃), as shown in Figure 6

Preprints (www.preprints.org) | NOT PEER-REVIEWED | Posted: 23 January 2018 doi:10.20944/preprints201801.0208.v1

Peer-reviewed version available at Energies 2018, 11, 595; doi:10.3390/en11030595

156

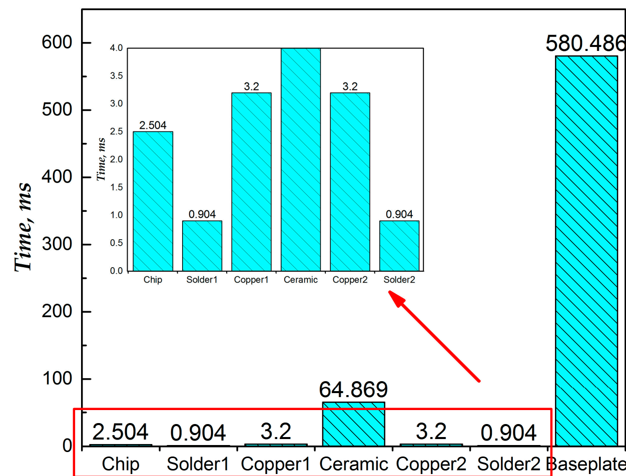

157 **Figure 6.** Time to reach steady-state of each layer.

158 According to the analysis of the data available in the figures, the times of the ceramic layer and
159 the baseplate are much longer than those of the other layers. The much longer heat transfer time is in
160 these two layers than in the other layers reduces the predictive performance of the transient junction
161 temperature in the inner layer structures of thermal model network, thereby degrading the overall
162 performance of capturing the transient junction temperature of the IGBT power module. To improve
163 the performance of the lumped Cauer-type thermal network model, the prediction accuracy can be
164 improved by the fine stratification of the ceramic layer and the baseplate layer. Equation (8) shows
165 that, with the increase of the number of layers, the thermal resistance and thermal capacitance
166 decrease with a trend of positive ratio function, and the time constant of new sublayer decreases with
167 a trend of quadratic. According to equation (10), the ceramic layer and the baseplate layer are divided
168 into several smaller sublayers that can reach the steady-state in a shorter period, and the time of each
169 layer after the re-division is in the same level, ensuring the smaller time span to required achieve the
170 optimization of the thermal network model performance. The data in figure [5-6] can be calculated
171 by equations (5), (6) and (10). The ceramic layer can be divided into 3 sublayers and the copper
172 baseplate can be divided into 4 sublayers to ensure the time of all layers can be kept at the same level.
173 In addition, the transient temperature difference in milliseconds is determined by the thermal
174 behaviour of chips. To better express the transient characteristics, chips are divided into 3 layers to
175 improve the transient performance of the Cauer-type models.

176 Redefining the stratification of the Cauer-type model of IGBT can effectively improve the
177 performance of capturing the dynamic junction temperature changes. The proposed multi-layered
178 thermal network model is compared with the conventional model, and the results are shown below
179 in Figure 7.

180

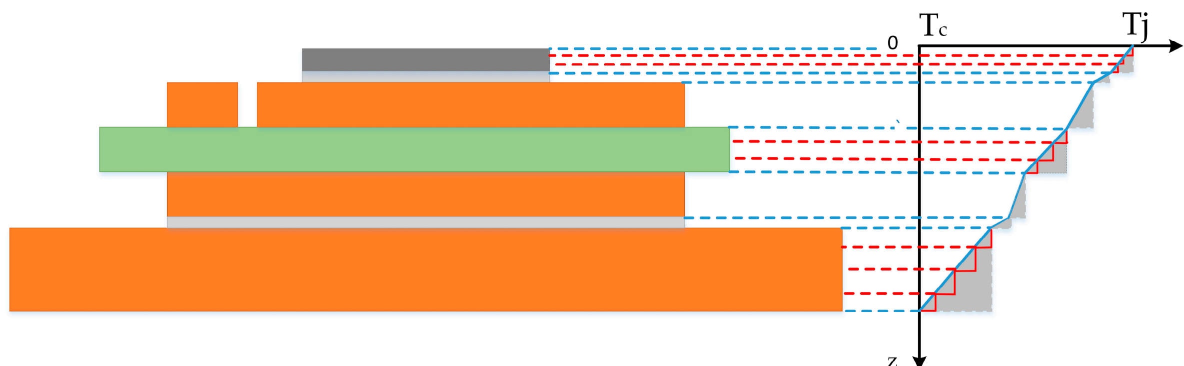

181 **Figure 7.** Comparison of two models.

Preprints (www.preprints.org) | NOT PEER-REVIEWED | Posted: 23 January 2018 doi:10.20944/preprints201801.0208.v1

Peer-reviewed version available at Energies 2018, 11, 595; doi:10.3390/en11030595

182 Analysis of Figure 7 shows that the method of subdividing the layer structure not only effectively improves the performance of the model in capturing the transient junction temperature but also largely reduces the error caused by ignoring the slope of the temperature distribution of the layers, that is the triangular area, thus achieving more accurate calculation of the heat inside each layer, thereby ensuring the accuracy of extracting thermal capacitance parameters of the model to accurately predict the transient junction temperature. Therefore, the improved Cauer-type thermal network model has been effectively improved in the prediction performance of transient junction temperature.

190 From the above, the Cauer-type thermal network model established on the basis of the proposed method, the performance of conventional Cauer-type model is optimized both in predicting the transient junction temperature and the steady-state junction temperature accuracy of the IGBT power module; remarkable results have been achieved.

194 3. Simulation validation

195 A commercial IGBT module SKM75GB12T4 made by SEMIKRON company is studied to verify the effectiveness of the proposed method. According to the geometric information provided in Table 1 and the material properties of each layer, the finite element analysis (FEA) model of the IGBT module in PRO/ENGINEER software is established, as shown in Figure 8.

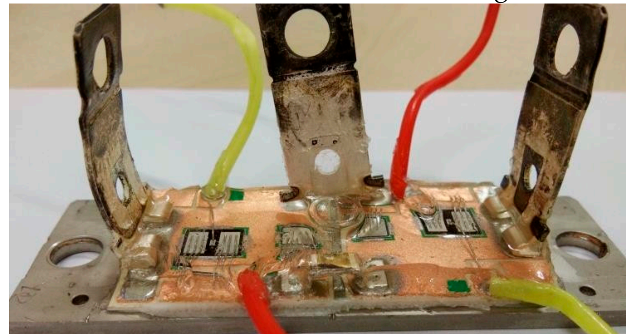

199
200 (**a**)

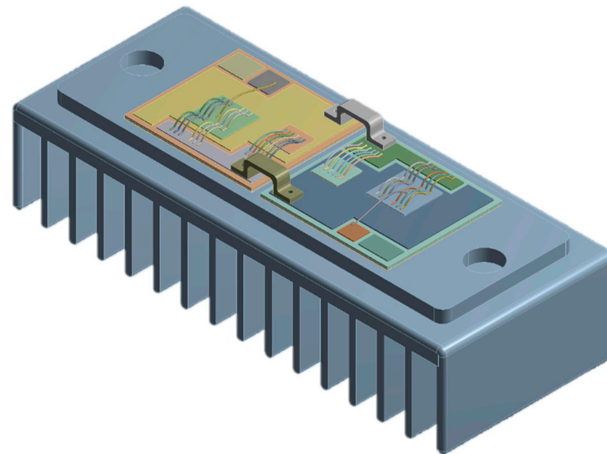

201
202 (**b**)

203 **Figure 8.** (**a**) IGBT module; (**b**) FEA model with a cold plate.

204 In the FEA model, the heat sink is simplified as an aluminium block, the bottom surface of the heat sink is set as a heat dissipative surface and the temperature of the bottom is set as a constant. The power loss is generated inside the chip near the surface; thus, the power loss is simulated on the chip surface, and the power loss set is shown in Figure 9. The temperature distribution of the IGBT module is obtained as shown in Figure 10. Therefore, the temperature information of different layers of the IGBT power module can be accurately mastered by the finite element model.

Preprints (www.preprints.org) | NOT PEER-REVIEWED | Posted: 23 January 2018 doi:10.20944/preprints201801.0208.v1

Peer-reviewed version available at Energies 2018, 11, 595; doi:10.3390/en11030595

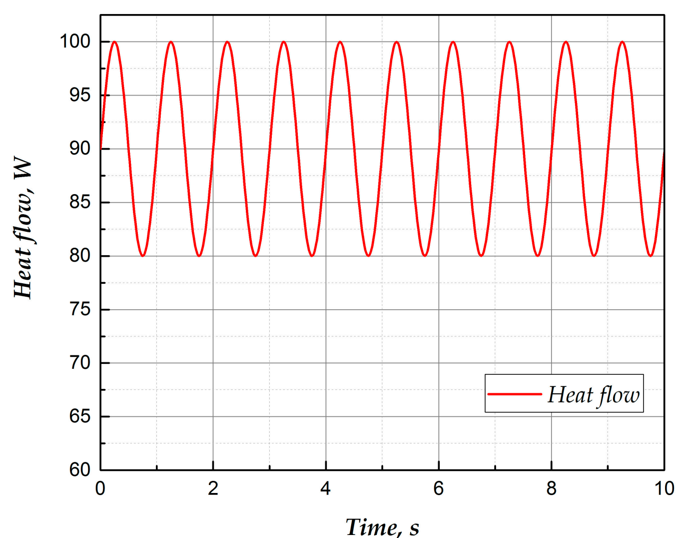

210
211 **Figure 9.** The input of heat flow.

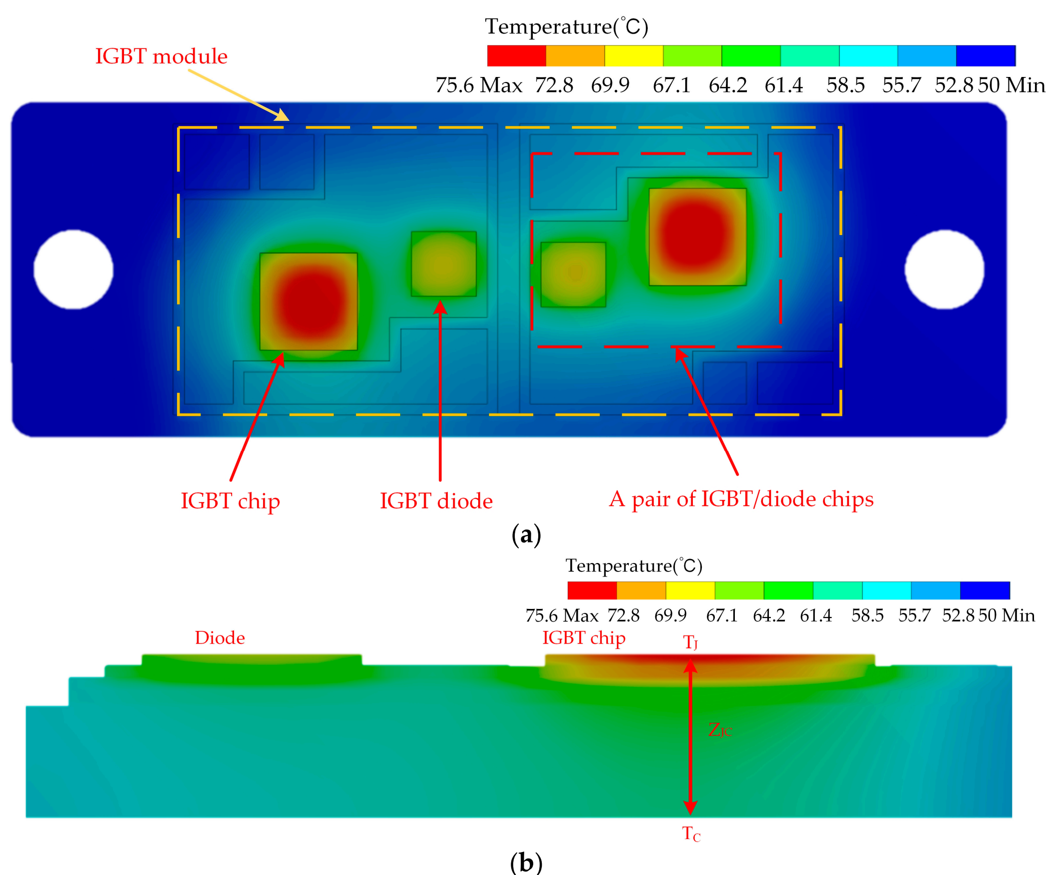

212
213
214
215
216 **Figure 10.** Temperature distribution in IGBT: (**a**) vertical view; (**b**) cross-sectional view.

217 On this basis, the conventional Cauer-type thermal network model and the improved thermal
218 network model are simulated, and the power loss, case temperature and ambient temperature as
219 input parameters are input to obtain the temperature curve of each module of IGBT power module.
220 The forecast results of junction temperature are compared with the results in the finite element
221 analysis model. The comparison results are shown in Figure 11.

Preprints (www.preprints.org) | NOT PEER-REVIEWED | Posted: 23 January 2018 doi:10.20944/preprints201801.0208.v1

Peer-reviewed version available at Energies 2018, 11, 595; doi:10.3390/en11030595

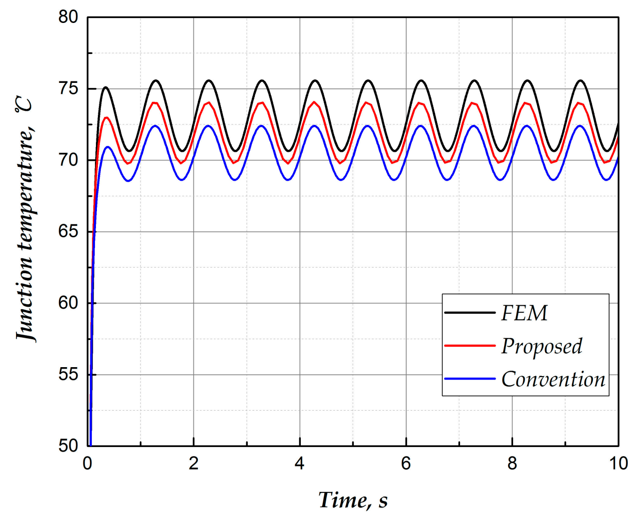

(a)

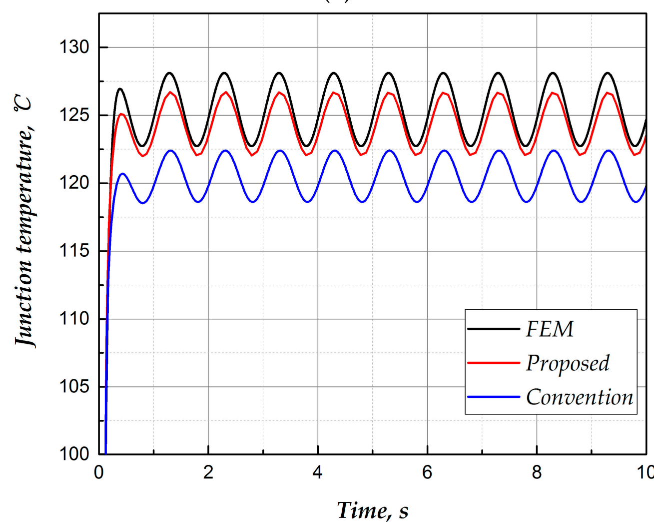

(b)

Figure 11. Junction temperature T_j as a function of time for the SKM75GB12T4 module during the variable heat flow test estimated from two thermal models: (**a**) the ambient temperature is 50℃; (**b**) the ambient temperature is 100℃.

Table 2. Comparison of two models.

Model	Peak-to-valley value(℃)	Average rate of change(℃/s)
FEM	4.99; 5.38	9.98; 10.76
Improved	4.35; 4.96	8.7; 9.92
Convention	3.68; 3.71	7.36; 7.42

The details of the simulation of Figure 11 are presented in Table 2. In a period of junction temperature fluctuation, the peak-to-valley value in the FEM model is 4.99℃ and 5.38℃ for 50 °C and 100 °C, respectively. The peak-to-valley value of the improved Cauer-type model is 4.35℃ and 4.96℃ for 50 °C and 100 °C respectively. However, the peak-to-valley value of the conventional Cauer-type model is 3.68℃ and 3.71℃ for 50 °C and 100 °C, respectively. Therefore, the average change rate of junction temperature of the improved Cauer-type model is closer to the change rate of the junction temperature in the FEM model, showing that the modified Cauer-type model effectively improves the predictive performance of transient temperature. Overall, the junction temperature value of the Cauer-type thermal network model is always greater than that of the conventional Cauer-type model and is closer to the predicting junction temperature in the FEM. Moreover, in the different ambient temperatures, the deviation prediction of the junction temperature from the improved

Preprints (www.preprints.org) | NOT PEER-REVIEWED | Posted: 23 January 2018 doi:10.20944/preprints201801.0208.v1

Peer-reviewed version available at *Energies* **2018**, *11*, 595; doi:10.3390/en11030595

241 Cauer-type model proposed in this paper is always kept in a small range, in good agreement with
242 the results from the FEM model, indicating that the improved Cauer-type model has excellent
243 prediction performance of steady-state junction temperature. With the continuous change of the
244 working state of the IGBT power module, the junction temperature is increasing. The higher junction
245 temperature will lead to the decrease of material thermal conductivity, leading to the increase of
246 thermal resistance inside the package. Similarly, with the increase of junction temperature caused by
247 the influence of specific heat capacity, the thermal capacitance in the package also increases. Thus,
248 the increase of thermal resistance and thermal capacitance is the main reason for the difference
249 between both of them in the predicted steady-state junction temperature. Moreover, with the increase
250 of thermal capacitance and thermal resistance, the model cannot accurately simulate the law of the
251 junction temperature, mainly including switching process, rise and fall time and so on. On the basis
252 of guaranteeing the precision of prediction of steady-state junction temperature, the reasonable
253 layering allows the improved Cauer-type model to realize the accurate simulation of the operating
254 law of the junction temperature.
255 In summary, the improved Cauer-type thermal network model proposed in this paper modifies
256 the conventional Cauer-type model from two aspects, namely, prediction of the transient junction
257 temperature and prediction of the steady-state junction temperature, and the two aspects of
258 optimization achieved notable results. The establishment of the temperature adaptive Cauer-type
259 thermal network model is completed.

260 **4. Experimental validation**

261 *4.1. Experiment setup*

262 The improved method is further verified by experimental studies in accordance with Figure 12.
263 Figure 12 shows the experimental setup, which consists of a high-DC power for supplying test
264 current, a gate driver for generating gate signal for the test IGBT module, a recorder for electrical
265 signal acquisition (such as V_{ce} and I_c), an infrared camera for real-time collection of the junction
266 temperature, a and National Instruments (NI) data acquisition instrument with a LabVIEW system
267 for acquiring the T_c, which is measured by using precise fine-wire thermocouple.

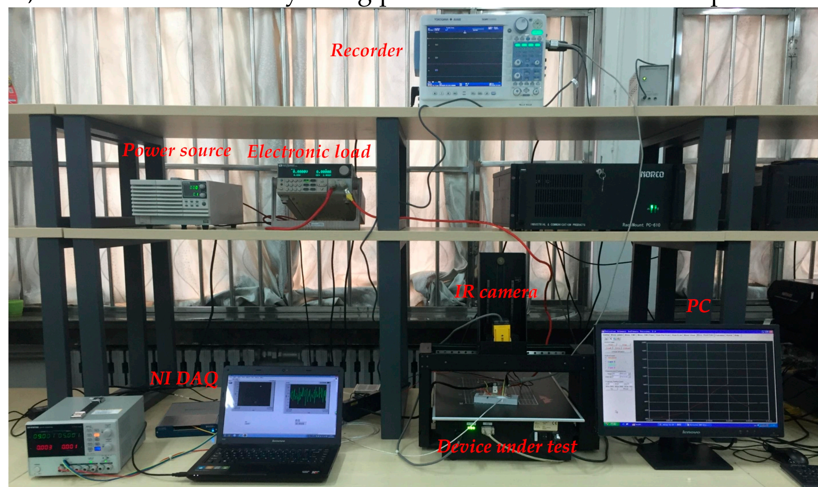

268
269 (a)

Preprints (www.preprints.org) | NOT PEER-REVIEWED | Posted: 23 January 2018 doi:10.20944/preprints201801.0208.v1

Peer-reviewed version available at Energies 2018, 11, 595; doi:10.3390/en11030595

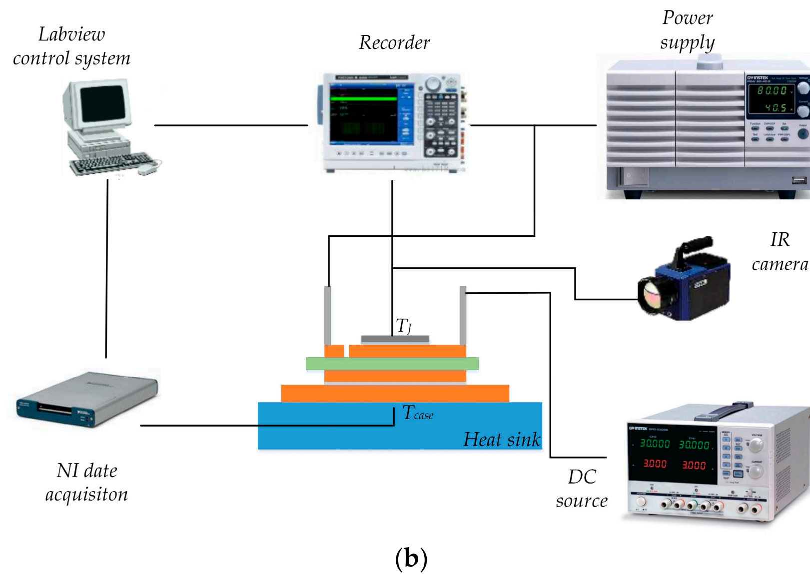

270
271 (b)

272 **Figure 12.** Experimental setup: (**a**) schematic; (**b**) actual setup.

273 *4.2 Variable current test*

274 On this basis, the thermal network models are examined; the upper surface temperature
275 distribution for the IGBT module obtained using the infrared imager is shown in Figure 13. To allow
276 the infrared camera accurately capture the junction temperature, the silicon gels from the surface of
277 the IGBT module should be removed deliberately and the camera should be aimed at the centre of
278 the chip.

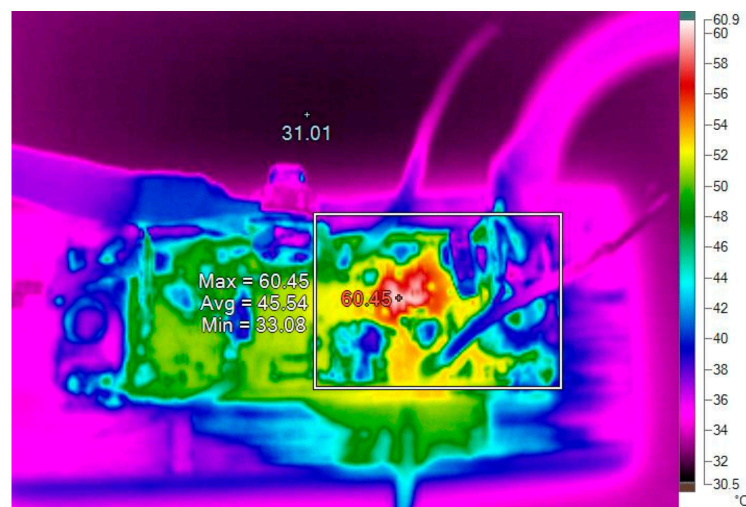

279

280 **Figure 13.** The temperature distribution of IGBT taken by the infrared imager.

281 In addition, the gate drive voltage is set as V_G=15 V to set the IGBT in a constant conduction
282 state. The current set is shown in Figure 14. The power loss of the IGBT, which will be integrated by
283 V_{ce} and I_c, is regarded as the input power unit of thermal network. Obtaining the real-time T_c by the
284 thermocouple will be taken as the baseplate temperature unit input of thermal network.

Preprints (www.preprints.org) | NOT PEER-REVIEWED | Posted: 23 January 2018 doi:10.20944/preprints201801.0208.v1

Peer-reviewed version available at Energies 2018, 11, 595; doi:10.3390/en11030595

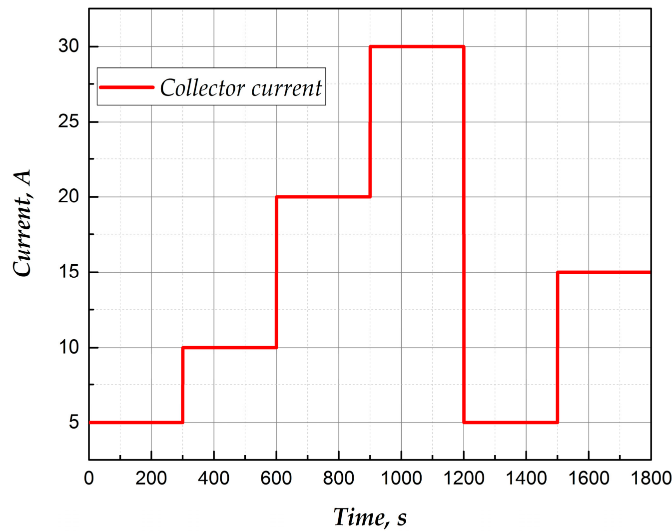

Figure 14. The input of the collector current.

Compared with experimental results, the results of the conventional Cauer-type model and the improved Cauer-type model are obtained, as shown in Figure 15.

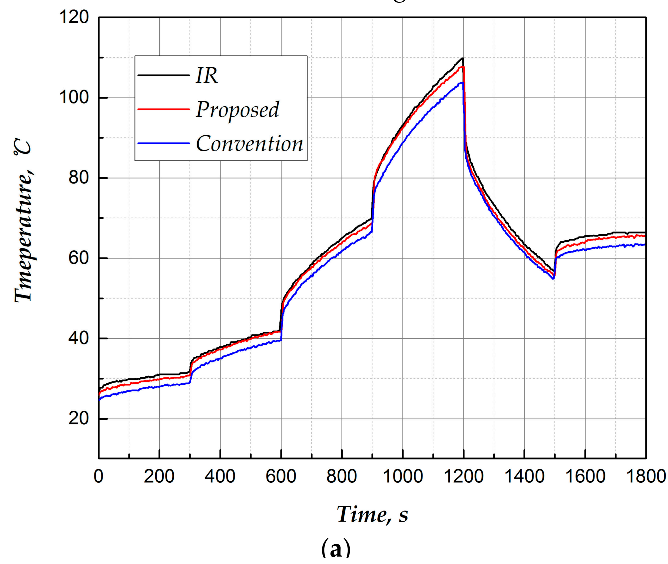

(a)

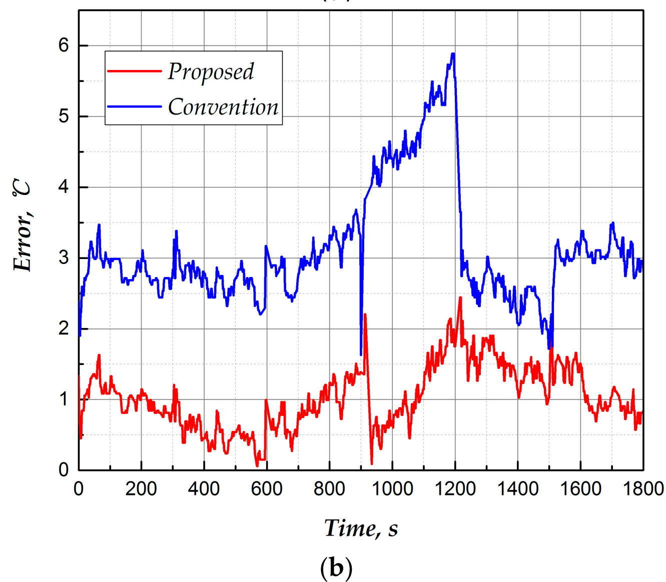

(b)

Preprints (www.preprints.org) | NOT PEER-REVIEWED | Posted: 23 January 2018 doi:10.20944/preprints201801.0208.v1

Peer-reviewed version available at *Energies* **2018**, *11*, 595; doi:10.3390/en11030595

Figure 15. Comparison of the junction temperature estimated by two models: (**a**)$T_j(t)$; (**b**) errors with respect to the IR camera.

The details of Figure 15 are given in Table 3. As the current changes, the junction temperature of the IGBT is constantly changing. Compared with the conventional Cauer-type model, the deviation of the prediction of the junction temperature from that of the improved Cauer-type model proposed in this paper is always kept in a small range. Figure 15(b) compares the values of the junction temperature estimation errors of the conventional Cauer-type model and those of the improved Cauer-type model with respect to the results obtained by the IR camera. As demonstrated in Figure 15(b), the maximum deviation between the actual temperature and the junction temperature predicted by the improved Cauer-type thermal network is 2.34℃, whereas the maximum deviation of the conventional Cauer-type model is 5.88℃, which is approximately 2.5 times that of the improved Cauer-type model. After optimization, the error fluctuation $\Delta Error_c$ is 2.3℃ and 4.25℃ for the Cauer-type model and the conventional model, respectively, indicating that the improved Cauer-type model performs better in transient junction temperature prediction. Moreover, the average deviation of the improved Cauer-type model is only 33% of the conventional model, indicating that the prediction performance of steady-state junction temperature is effectively improved.

Table 3. Comparison of the two models with respect to the IR camera.

Model	Maximum deviation(℃)	Error fluctuation(℃)	Average deviation(℃)
Improved	2.34	2.30	1.03
Convention	5.88	4.25	3.13

From the above, the improved Cauer-type thermal network proposed in this paper effectively corrects the conventional Cauer-type thermal network from two aspects, namely, prediction of the transient junction temperature and prediction of the steady-state junction temperature, making the improved Cauer-type model predicted junction temperature curve close to the experimental data. Moreover, the improved Cauer-type model also has excellent prediction performance in variable current conditions. As the result, the law of junction temperature can be captured accurately. The establishment of temperature-adaptive Cauer-type thermal network model is completed.

5. Conclusions

In this paper, a method to improve the conventional Cauer-type thermal network model of an IGBT by considering both the temperature influence on the extraction of parameters and the error caused by physical structure was presented. Furthermore, the efficiency of this model was verified through simulation and experiment on a commercial IGBT module. The improved Cauer-type thermal network modifies the convention model both in prediction of the transient junction temperature and in the steady-state junction temperature accuracy. Both modified models have remarkable effects, indicating the excellent prediction performance of the junction temperature. Based on the high-precision prediction performance, the temperature adaptive Cauer-type model was established.

6. Acknowledgements

The authors wish to acknowledge the financial support of National Key R&D Program of China (No. 2017YFB0102500) and Tianjin Natural Science Foundation of China (No. 17JCYBJC21300). Thanks to Prof. Hurley William Gerard from Electrical Engineering with the National University of Ireland, Galway, Ireland.

References

1. Blaabjerg, F.; Ma, K. Future on power electronics for wind turbine systems. *IEEE Trans. Power Electr.* **2013**, *1(3)*, 139-152.

Preprints (www.preprints.org) | NOT PEER-REVIEWED | Posted: 23 January 2018 doi:10.20944/preprints201801.0208.v1

Peer-reviewed version available at Energies 2018, 11, 595; doi:10.3390/en11030595

335 2. Ji, B.; Pickert, V.; Cao, W. In situ diagnostics and prognostics of wire bonding faults in IGBT modules for
336 electric vehicle. *IEEE Trans. Power Electr.* **2013**, *28*, 5568-5577
337 3. Xu, Z.; Li, M.; Wang, F. Investigation of Si IGBT operation at 200℃ for traction application. *IEEE Trans.*
338 *Power Electr.* **2013**, *28*, 2604-2615
339 4. Cao, W.; Mevrow, B.; Atkinson, G.J. Overview of electric motor technologies used for more electric
340 aircraft(MEA). *IEEE Trans. Ind. Electr.* **2012**, *59*, 3523-3531
341 5. Senturk, O.; Helle, L.; Munk-Nielsen, S. Power capability investigation based on electrothermal models of
342 press-pack IGBT three-level NPC and ANPC VSCs for multimegawatt wind turbines. *IEEE Trans. Power*
343 *Electr.* **2012**, *27*, 3195-3206
344 6. Li, H.; Hu, Y.; Liu, S. An improved thermal network model of the IGBT module for wind power converters
345 considering the effects of base plate solder fatigue. *IEEE Trans. Device and Materials Reliability.* **2016**, *16*, 570-
346 575
347 7. Gong, X.; Ferreira, J.A. Comparison and reduction of conducted EMI in SiC JFET and Si IGBT-based motor
348 drives. *IEEE Trans. Power Electr.* **2014**, *29*,1757-1767
349 8. Shaoyong, Yang.; Angus, B.; Philip, M.; Dawei, X.; Li, R.; Peter, T. An industry-based survey of reliability
350 in power electronic converter. *IEEE Trans. Ind. Appl.* **2011**, *47*, 3151-3157
351 9. Ismail, M.A.; Tamchek, N. A fiber bragg grating—bimetal temperature sensor for solar panel inverters.
352 *Sensors*. **2011**, *11*, 8665-8673
353 10. Liu, Z.; Mei, W.; Zeng, X.; Zhou, X. Remaining useful life estimation of insulated gate bipolar
354 transistors(IGBTs) based on a novel volterra k-nearest neighbor optimally pruned extreme learning
355 machine(VKOPP) model using degradation data. *Sensors*. **2017**, *17*, 2524-2546
356 11. Dupont, L.; Avenas, Y.; Jeannin, P-O. Comparison of junction temperature evaluations in a power IGBT
357 module using an IR camera and three thermosensitive electrical parameters. *IEEE Trans. Ind. Appl.* **2013**, *49*,
358 1599-1608
359 12. Khatir, Z.; Dupont, L.; Ibrahim, A. Investigation on junction temperature estimation based on junction
360 voltage measurements. *Microelectron. Reliab.* **2010**, *50*, 1506-1510
361 13. Cao, X.; Wang, T. Characterization of lead-free solder and sintered nano-silver die-attach layers using
362 thermal impedance. *IEEE Trans. Compon. Packag. Manuf. Technol.* **2011**, *1*, 495-501
363 14. Avenas, Y.; Dupont, L.; Khatir, Z. Temperature measurement of power semiconductor devices by thermos-
364 sensitive electrical parameters—A review. *IEEE Trans. Power Electr.* **2012**, *27*, 3081-3092
365 15. Luo, H.; Chen, Y.; Sun, P. Junction temperature extraction approach with turn-off delay time for high-
366 voltage high-power IGBT modules. *IEEE Trans. Power Electr.* **2016**, *31*, 5122-5132
367 16. Perdersen, K.B.; Kristensen, P.K. Vce as early indicator of IGBT module failure mode. In Proceedings of the
368 IEEE Reliability Physics Symposium, Aalborg, Denmark, 2-6 April 2017; FA-1.1-FA-1.6
369 17. Shabany, Y. *Heat transfer: thermal management of electronics.*; CRC Press: France, Francis, 2010; pp.61-65, ISBN:
370 9781439814673
371 18. Chen, M.; Hu, A.; Yang, X. Predicting IGBT junction temperature with thermal network component model.
372 In Proceedings of the Asia-Pacific Power and Energy Engineering Conference, Washington, DC, USA, 25-
373 28 March 2011; pp.1-4
374 19. Ma, K.; He, N.; Liserre, M. Frequency-domain thermal modeling and characterization of power
375 semiconductor devices. *IEEE Trans. Power Electr.* **2016**, *31*, 7183-7193
376 20. Dutta, S.; Parkhideh, B.; Subhashish, D. Development of a predictive observer thermal model for power
377 semiconductor devices for overload monitoring in high power high frequency converters. In Proceedings
378 of Applied Power Electronics Conference and Exposition, Raleigh, NC, USA, 5-9 February 2012; pp.2305-
379 2310
380 21. Luo, Z.; Ahn, H. A thermal model for Insulated Gate Bipolar Transistor module. *IEEE Trans. Power Electr.*
381 **2004**, *19*, 902-907
382 22. Ma, K.; Liserre, M.; Blaabjerg, F.; Kerekes, T. Thermal loading and lifetime estimation for power device
383 considering mission profiles in wind power converter. *IEEE Trans. Power Electr.* **2015**, *30*, 590-602
384 23. Bahman, A.S.; Ma, K.; Ghimire P. A 3-D-Lumped thermal network model for long-term load profiles
385 analysis in high-power IGBT modules. *IEEE J. Emerg. Select. Topic Power Elect*. **2016**, *4*, 1050-1063
386 24. Tang, Y.; Ma, H. Dynamic electrothermal model of paralleled IGBT modules with unbalanced stray
387 parameters. *IEEE Trans. Power Electr.* **2017**, *32*, 1385-1399

Preprints (www.preprints.org) | NOT PEER-REVIEWED | Posted: 23 January 2018 doi:10.20944/preprints201801.0208.v1

Peer-reviewed version available at *Energies* **2018**, *11*, 595; doi:10.3390/en11030595

388 25. Tian, B.; Qiao, W.; Wang Z. Monitoring IGBT's health condition via junction temperature variations. In
389 Proceedings of Applied Power Electronics Conference and Exposition, Lincoln, NE, USA, 16-20 March 2014,
390 pp.2550-2555
391 26. Batard, C.; Ginot, N.; Antonios, J. Lumped dynamic electrothermal model of IGBT module of inverters.
392 *IEEE Trans. Compon. Packag. Manuf. Technol.* **2015**, *5*, 355-364
393 27. Yun, C.; Malberti, P.; Ciappa, M.; Fichtner, W. Thermal component model for electrothermal analysis of
394 IGBT module systems. *IEEE Trans. Advanced Packag.* **2001**, *24*, 401-406
395 28. Material Home. Available online: http://www.efunda.com/materials/materials_home/materials.cfm
396 (accessed on 18 January 2018)
397 29. Du, B.; Hudgins, J.; Santi, E. Transient electrothermal simulation of power semiconductor devices. *IEEE*
398 *Trans. Power Electr.* **2010**, *25*, 237-248